

Hydrogen-mediated long-range magnetic ordering in Pd-rich alloy film

Wen-Chin Lin, Cheng-Jui Tsai, Han-Yuan Huang, Bo-Yao Wang, Venkata Ramana Mudinepalli, and Hsiang-Chih Chiu

Citation: [Applied Physics Letters](#) **106**, 012404 (2015); doi: 10.1063/1.4905463

View online: <http://dx.doi.org/10.1063/1.4905463>

View Table of Contents: <http://scitation.aip.org/content/aip/journal/apl/106/1?ver=pdfcov>

Published by the [AIP Publishing](#)

Articles you may be interested in

[Long range magnetic ordering with giant magnetic moments in Pt doped NiMn thin films](#)

J. Appl. Phys. **105**, 07D536 (2009); 10.1063/1.3075858

[Structural and magnetic properties of a chemically ordered face-centered-cubic \(111\) Mn alloy film](#)

J. Appl. Phys. **99**, 08N504 (2006); 10.1063/1.2163324

[Long-range order and short-range order study on CoCrPt/Ti films by synchrotron x-ray scattering and extended x-ray absorption fine structure spectroscopy](#)

J. Appl. Phys. **91**, 7182 (2002); 10.1063/1.1448799

[High perpendicular anisotropy and magneto-optical activities in ordered Co₃Pt alloy films](#)

J. Appl. Phys. **83**, 6527 (1998); 10.1063/1.367917

[Magneto-optical spectra of long range chemically ordered FePd\(001\) alloy films](#)

J. Appl. Phys. **82**, 4449 (1997); 10.1063/1.366254

The advertisement features a red and white color scheme. On the left, text reads 'Confidently measure down to 0.01 fA and up to 10 PΩ' and 'KeySight B2980A Series Picoammeters/Electrometers'. A red button with white text says 'View video demo'. On the right, there is an image of the B2980A device and the KeySight Technologies logo.

Hydrogen-mediated long-range magnetic ordering in Pd-rich alloy film

Wen-Chin Lin,^{1,a)} Cheng-Jui Tsai,¹ Han-Yuan Huang,¹ Bo-Yao Wang,^{2,b)}
 Venkata Ramana Mudinepalli,¹ and Hsiang-Chih Chiu¹

¹Department of Physics, National Taiwan Normal University, Taipei 116, Taiwan

²Department of Physics, National Changhua University of Education, Changhua 500, Taiwan

(Received 19 October 2014; accepted 21 December 2014; published online 6 January 2015)

The effect of hydrogenation on a 14 nm $\text{Co}_{14}\text{Pd}_{86}/\text{Al}_2\text{O}_3(0001)$ thin film was investigated on the basis of the magneto-optical Kerr effect. After exposure to H_2 gas, the squareness of the hysteresis loop showed a large transition from approximately 10% to 100% and the saturation Kerr signal was reduced to nearly 30% of the pristine value. The reversibility of the transition was verified and the response time was within 2–3 s. These observations indicate that the hydride formation transformed the short-range coupled and disordered magnetic state of the $\text{Co}_{14}\text{Pd}_{86}$ film to a long-range-ordered ferromagnetic state and induced appreciable decrease in the magnetic moment. The enhanced long-range-ordering and the reduction of the magnetic moment were attributed to the change of electronic structure in $\text{Co}_{14}\text{Pd}_{86}$ with hydrogen uptake. © 2015 AIP Publishing LLC.

[<http://dx.doi.org/10.1063/1.4905463>]

The manipulation of magnetic properties, particularly in metallic materials, through the reversible modification of the crystalline structure or electronic structure is challenging and warrants study, from the viewpoint of both fundamental physics and technical applications.^{1–4} In our previous studies, the combination of Pd with magnetic transition metals provided an opportunity to modulate the magnetism, because Pd is an efficient catalyst in the dissociation of hydrogen molecules and the presence of Pd atoms can also help to stabilize hydrogen bounding to transition metals.^{5–12} The palladium-hydrogen system has attracted intensive research efforts in physical chemistry as a model system because of its high storage capacity, its high sensitivity and selectivity to H_2 gas, and its ability to easily release hydrogen at room temperature.¹³ Our previous reports on the effect of hydrogenation on Pd/Fe, Co, and Ni bilayers showed the significant enhancement of the magneto-optical Kerr signal, but without any observable modification of the intrinsic magnetic properties, such as the shape of the magnetic hysteresis loop and magnetic coercivity.¹⁴ In an annealed Pd/Co/Pd trilayer and a $[\text{Co}/\text{Pd}]_{12}$ multilayer, the hydrogenation induced modulation of the magnetism was observed clearly because of the enhanced interface effect.^{15–18} Based on these findings, we expected to observe appreciable magnetic modulation in Pd-rich magnetic alloy thin film; such materials would be useful for fabricating gas sensors.^{19–21} Thus, in this study, the effect of hydrogenation on the magnetic properties of $\text{Co}_{14}\text{Pd}_{86}$ was investigated. Reversible and appreciable modulation of the magnetism was demonstrated and analyzed for discussion.

The $\text{Co}_{14}\text{Pd}_{86}$ alloy thin films were deposited on an $\text{Al}_2\text{O}_3(0001)$ substrate through co-evaporation of Co and Pd from two e-beam heated evaporators.^{15,16} The alloy composition was calibrated using Auger electron spectroscopy. Atomic force microscopy was used to investigate the surface

morphology. The magnetic properties were measured at room temperature by using the magneto-optical Kerr effect (MOKE) in both perpendicular and in-plane geometry.^{15,16} The MOKE chamber was either pumped to a vacuum of 5×10^{-3} mbar or filled with H_2 gas at various pressures to investigate the effect of hydrogenation on the magneto-optical and magnetic properties of $\text{Co}_{14}\text{Pd}_{86}$.

Because the Co composition is only 14%, the $\text{Co}_{14}\text{Pd}_{86}$ alloy films on $\text{Al}_2\text{O}_3(0001)$ reveal the face-centered-cubic structure, the same as bulk Pd, with the (111) texture.¹⁵ Figure 1 shows the measured perpendicular and in-plane MOKE hysteresis loops of the 14 nm $\text{Co}_{14}\text{Pd}_{86}/\text{Al}_2\text{O}_3(0001)$ thin film. Observable hysteresis loops were obtained for both directions, suggesting a canted magnetization in the $\text{Co}_{14}\text{Pd}_{86}$ alloy film. In air and in a vacuum of 5×10^{-3} mbar, the $\text{Co}_{14}\text{Pd}_{86}$ film exhibited the same hysteresis loops, as shown by the black solid lines in Figs. 1(a) and 1(b). Both perpendicular and in-plane hysteresis loops showed a low coercivity and a small remanence.^{16,17} The low remanence, as compared with the saturation signal, indicates weak and short-range magnetic coupling in the Pd-rich alloy film. Various noble metals weakly diluted with transition metal ions have been identified as classical spin glass materials, in which no conventional long-range order can be established, and the spins are aligned in random directions.²² When the magnetic field was switched off, the well-aligned magnetic moment became disordered, leading to a small remanence magnetization. The pristine magnetic hysteresis loops of the $\text{Co}_{14}\text{Pd}_{86}$ film, measured in air and in a vacuum, actually show the spin-glass-like magnetic behavior.

As shown in Figs. 1(a) and 1(b), a series of MOKE measurements were recorded for the detection of the effect of hydrogenation on the magnetic properties of the $\text{Co}_{14}\text{Pd}_{86}$ film for different H_2 gas pressures. After exposure to H_2 gas, significant changes were observed from the hysteresis loops. The experiment results are summarized in Fig. 2. The magnetic coercivity H_c , the squareness of the hysteresis loop (i.e., remanence M_r /saturation M_s), and the saturation Kerr

^{a)}E-mail: wclin@ntnu.edu.tw

^{b)}E-mail: bywang1735@cc.ncue.edu.tw

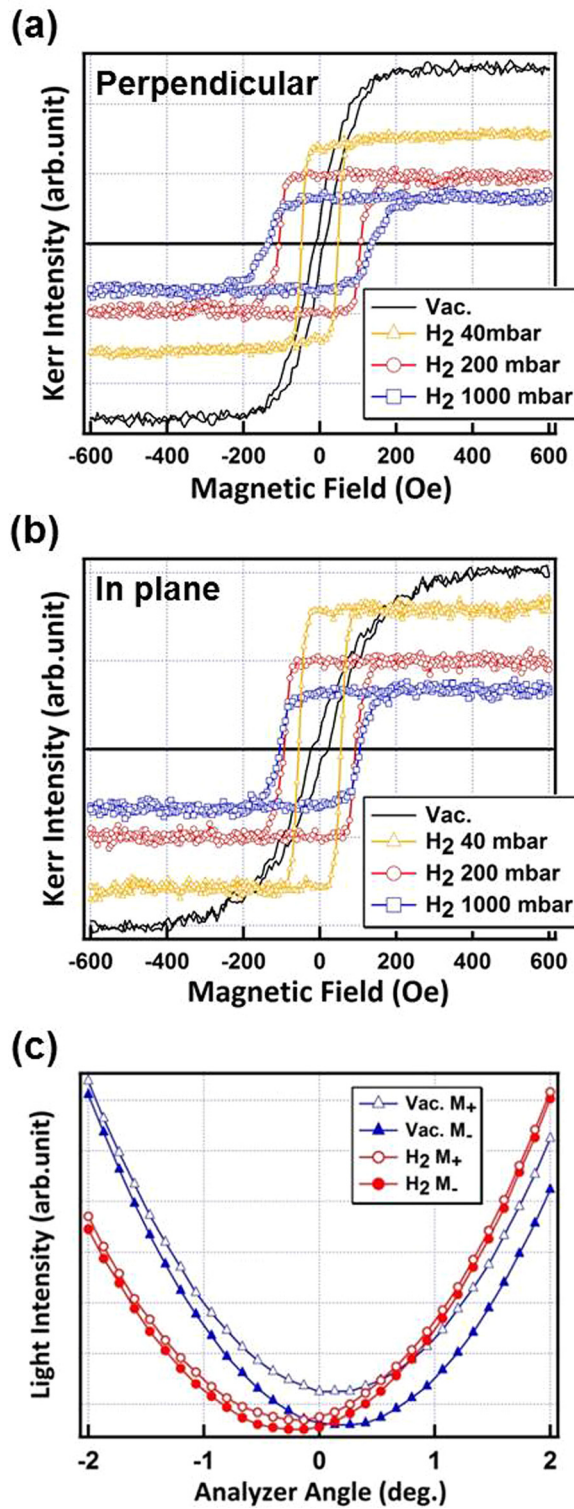


FIG. 1. Magnetic hysteresis loops of 14 nm $\text{Co}_{14}\text{Pd}_{86}/\text{Al}_2\text{O}_3(0001)$ measured using the magnetooptical Kerr effect: (a) for the perpendicular direction and (b) for the in-plane direction. The hysteresis loops were measured in a vacuum (5×10^{-3} mbar) and for H_2 gas pressure of 40–1000 mbar. (c) The light intensity $I_{\pm m}$ measured in the vacuum and for 1000 mbar H_2 gas is plotted as a function of the analyzer angle ϕ . The solid lines are the curves fitted using Eq. (1).

signal normalized by the pristine value in a vacuum are plotted as a function of the H_2 gas pressure, which ranges from a vacuum of 5×10^{-3} mbar to 1000 mbar H_2 . After exposure to 40 mbar H_2 , the perpendicular H_c increased by a factor of 3, from 15 Oe to approximately 45 Oe. With an increasing

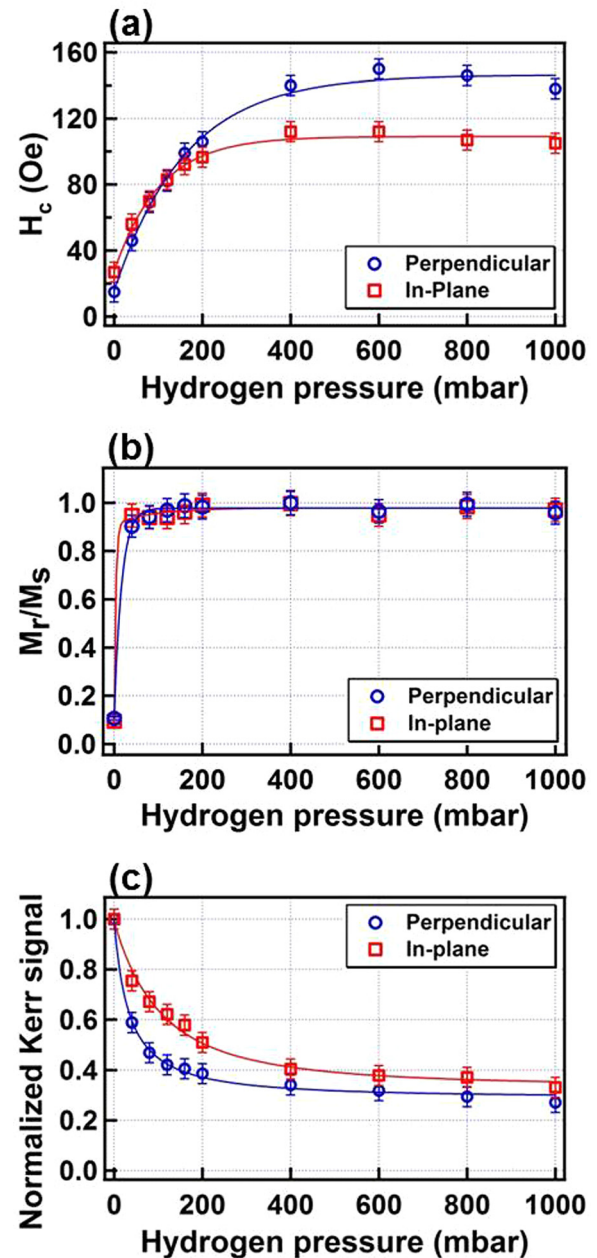


FIG. 2. (a) Magnetic coercivity (H_c), (b) squareness (M_r/M_s), and (c) normalized Kerr saturation signal of the MOKE hysteresis loops of 14 nm $\text{Co}_{14}\text{Pd}_{86}/\text{Al}_2\text{O}_3(0001)$. The data obtained were plotted as a function of the H_2 gas pressure. The lines are a visual guide.

H_2 gas pressure, the perpendicular H_c monotonously increased, reaching a maximum of 150 Oe for 600 mbar H_2 . The perpendicular H_c then decreased slightly to 138 Oe for 1000 mbar H_2 . A similar trend was observed for the in-plane H_c , which increased from 27 Oe in a vacuum, reached a maximum of 112 Oe for 400 mbar H_2 , and then slightly decreased to 105 Oe for 1000 mbar H_2 . In addition to the marked increase in H_c , as shown in Fig. 2(b), the squareness M_r/M_s drastically changed from 10% in a vacuum to nearly 90% for 40 mbar H_2 . The squareness retained 100% with a further increase in the H_2 pressure. Because a sharp transition of squareness occurred in both perpendicular and in-plane directions, we can conclude that the enhancement of squareness was not due to the reorientation of the easy axis. Instead, this observation clearly indicates a transition from a

disordered short-range magnetic coupling state to a long-range-ordered ferromagnetic state. The disordered magnetic state for the dilute $\text{Co}_x\text{Pd}_{1-x}$ alloy is not a spurring result. Noble metals weakly diluted with transition metal ions, such as Fe or Mn, are the “classical” spin glass materials, in which the interactions between the magnetic moments are “in conflict” with each other, due to some frozen-in structural disorder.²² For example, study of Sandlund *et al.* also showed the spin glass behavior of a 3 nm Cu(13.5 at. % Mn) film.²³ The presence of hydrogen atoms in the interstitial space between Co and Pd atoms played a critical role in causing the transition to long-range magnetic coupling.

In the study of Akamaru *et al.*, the slight change of Co composition in Co-Pd alloy can significantly change the absorption capacity of hydrogen. This indicates that Pd-H bonding is stronger and more stable than the Co-H bonding in the alloy sample.¹² In the Co-Pd alloy, the large number of hydrogen bonded by Pd will bring in more contact between the H and Co. The Pd-H and Co-H hydride formation unavoidably leads to charge transfer and the pronounced change of electronic structure accordingly. Many theoretical calculations have been performed and many experimental studies also point out that the hydrogenation of transition metals can change the magnetic susceptibility, magnetic interlayer coupling, and resistivity, which are mainly due to the change of electric structure.^{10,11,24,25}

In the Pd-rich alloy film, the magnetic moment is mainly located at the Co atoms, which are surrounded by the polarized Pd atoms. The indirect exchange interaction between Co moments is transferred through the conduction electrons in Pd medium.²² The collective behavior is thus determined by this RKKY interaction (Ruderman and Kittel, 1954; Kasuya, 1956; Yosida, 1957).²² The uptake of H may change the characteristics of the conduction electrons in Pd and accordingly the RKKY interaction, leading to the transformation of magnetic behavior. For example, Klose *et al.* reported that the magnetic coupling of a $(26 \text{ \AA} \text{ Fe}/15 \text{ \AA} \text{ Nb}) \times 18$ multilayer was changed in a continuous and reversible way by introducing hydrogen into the sample.²⁴ The change of the magnetic coupling was attributed to a change of the effective Fermi wave vector in Nb due to hydrogen uptake.²⁴ Similarly, the interlayer ordering between ferromagnetic Fe layers in Fe/V (001) superlattices is switched initially parallel to antiparallel, as well as antiparallel to parallel, upon introducing hydrogen to the V layers.²⁵ The major cause of the interlayer coupling transitions is most likely the distortion of the Fermi surface in the V layers.²⁵ In contrast of the above-mentioned multilayer systems, our experimental results show a drastic transformation of magnetic coupling in a simple diluted alloy thin film, which is also attributed to the hydrogen-induced modulation of the electronic structure in Pd.

In Fig. 2(c), the saturation Kerr signal normalized by the pristine value in a vacuum is plotted as a function of the H_2 pressure. The perpendicular measurements show that the saturation Kerr signal decreased to 60% for 40 mbar H_2 gas and then monotonously decreased to 27%. The in-plane measurements show that the saturation Kerr signal decreased to 75% for 40 mbar H_2 gas and then monotonously decreased to 33%. Despite the differing variation rates in the two

directions, the saturation Kerr signal eventually reached a stable level corresponding to $70 \pm 3\%$ reduction.

In the MOKE measurement, we focused a *p*-polarized 670-nm laser beam on the sample.^{15,16} An analyzer, comprising a linear polarizer oriented at a small angle ϕ from the *s*-axis and a photodiode, was used to detect the reflected beam. When a magnetic sample was used, the reflected beam was no longer purely *p*-polarized; instead, it comprised a *p*-component (E_p) and an *s*-component (E_s).²⁶ The ratio E_s/E_p is expressed as $\theta + i\epsilon$, where θ is the Kerr rotation and ϵ is the Kerr ellipticity. When ϕ is small, the measured light intensity I can be expressed as a parabolic function of ϕ as follows:^{15,16}

$$I_{\pm m} = |E_p|^2(\phi^2 + 2\theta_{\pm m}\phi + \theta_{\pm m}^2 + \epsilon_{\pm m}^2). \quad (1)$$

Figure 1(c) shows the light intensity of the $\text{Co}_{14}\text{Pd}_{86}$ film in a vacuum and for 1000 mbar H_2 gas. The light intensity $I_{\pm m}$ is plotted as a function of the analyzer angle ϕ for the positively (+*m*) and negatively (−*m*) magnetized sample; the magnetic field used for the magnetization was ± 600 Oe. The experimental data were fitted with the parabolic function of Eq. (1), and the fit is indicated by the solid lines in Figure 1(c). According to the fitting results, the reflectivity $|E_p|^2$ decreased to 93%, and the Kerr rotation angle $\theta_k = (\theta_{+m} - \theta_{-m})/2$ was substantially reduced to only 12% of the pristine value after exposure to 1000 mbar H_2 gas. Thus, reduction of Kerr signal is mainly due to the large decrease of Kerr rotation angle, rather than the reflectivity.

In our previous Pd/Fe, Co, Ni bilayer, and Pd/Co/Pd trilayer samples, the Kerr intensity is enhanced, similar to the previous report of Lederman *et al.*^{10,14} Lederman *et al.* mentioned that the thicker Pd overlayers increase the MO enhancement, with remarkably large enhancement of 50% for a Fe (4.1 nm)/Pd (10.0 nm) sample. This effect results from a change in the optical properties of the Pd overlayer.¹⁰ In contrast, the Kerr signal of the Co-Pd alloy film was reduced upon H_2 exposure, because Co-Pd alloy film is not a multilayer structure with a Pd overlayer. The reduction of Kerr signal actually implied the reduction of magnetic moment. Several previous studies have reported similar reduction effect upon H_2 absorption. The hydrogen absorption in Co/Pd multilayers decreases the total magnetization of the samples.¹⁷ The lack of measurable expansion during absorption indicates that these changes are primarily governed by modification of the electronic structure of the material.¹⁷ Besides, the magnetic susceptibility of the Pd-Co-H system abruptly decreased as the hydrogen content increased.¹² These behaviors were qualitatively interpreted in terms of the electronic structure of the Pd-Co-H system.¹² According to these previous experimental reports, the magnetic moment reduction is suggested to be the origin of the reduced Kerr signal measured in our experiment.

About the hydrogenation induced reduction of magnetic moment, previous experimental results performed by vibrating sample magnetometer and alternating-current magnetic susceptibility measurements also support our inference.^{12,17} Munbodh *et al.* reported the slight decrease of total magnetic moment in Co/Pd multilayers with H_2 absorption.¹⁷ In the experimental study on Co-H-Pd system carried out by

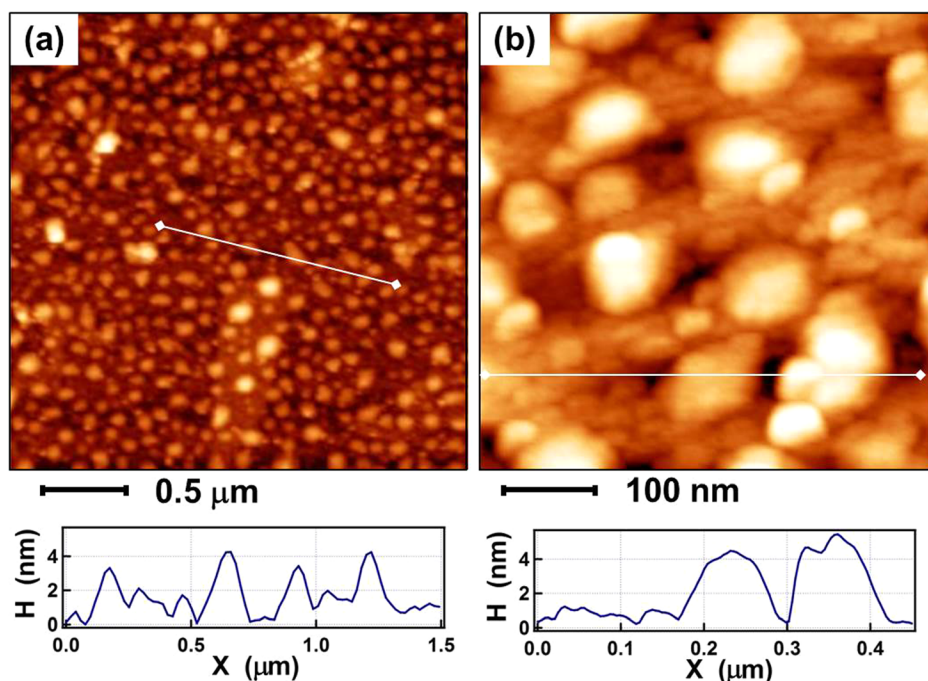


FIG. 3. Atomic force microscopy images of the 14 nm $\text{Co}_{14}\text{Pd}_{86}/\text{Al}_2\text{O}_3(0001)$ thin film shown at different scales. The indicated line profiles are plotted at the bottom of each image.

Akamaru *et al.*, the magnetic susceptibility of all the prepared Pd-Co alloys decreased upon hydrogen uptake.¹² Our MOKE measurement on the $\text{Co}_{14}\text{Pd}_{86}$ film revealed the more pronounced reduction of magnetism, because of the large Pd content around Co atoms. The mechanism for the hydrogenation induced moment reduction is still unexplained. Besides, as indicated in works of Kulriya *et al.*, the formation of defects in Pd significantly affects the magnetic properties of Pd nanoparticles.^{27,28} In our experiment, hydrogenation can possibly introduce structural defects due to lattice expansion and contraction on hydrogen absorption and desorption. This could be another reason for the change of the magnetic properties of Co-Pd alloy films. In the theoretical study of Gonzalez *et al.* of hydrogen effect on the electronic structure of Fe-Pd alloys, the H is stabilized by a narrow band of states below the *d* metal bands which is made up mostly of hydrogen based state ($>50\% \text{H}_{1s}$).¹¹ This feature state from H_{1s} may play an important role in the magnetic exchange coupling between Co and the nearest Pd. According to our experimental observations, the H_{1s} -mediation is suspected to weaken the coupling or even transfer it to an antiparallel coupling, leading to the reduction of magnetic moment.²⁹ Further spin-dependent theoretical calculation of the Co-H-Pd electronic structure may help to clarify the details.

The surface morphology of the 14 nm $\text{Co}_{14}\text{Pd}_{86}/\text{Al}_2\text{O}_3(0001)$ thin film was investigated through atomic force microscopy. As shown in Fig. 3(a), nano-clusters with heights of approximately 4 ± 1 nm and diameters of approximately 100 nm were randomly distributed on the surface. The average density was $46 \pm 4/\mu\text{m}^2$ and the average interdistance between neighboring clusters was approximately 150 nm. As shown in the magnified image in Fig. 3(b), the space between nano-clusters was relatively smooth and consisted of smaller clusters with heights of approximately 1 ± 0.5 nm and diameters of approximately 20 ± 10 nm. These surface nano-structures might originate from the strain relaxation or the defect distribution in the $\text{Co}_{14}\text{Pd}_{86}$ alloy

film, and they are responsible for the short time constant, within 2–3 s, of the hydrogenation process. In our previous study, $[\text{Co}/\text{Pd}]_{12}$ multilayer nano-dots exhibited a considerably fast hydrogenation response (within a few seconds), in contrast to the much longer response time of a $[\text{Co}/\text{Pd}]_{12}$ continuous film (2000–3000 s).¹⁸

Figure 4 shows the reversibility of the hydrogenation effect on the magnetism of the $\text{Co}_{14}\text{Pd}_{86}/\text{Al}_2\text{O}_3(0001)$ film. The MOKE measurement chamber was cyclically pumped to a vacuum and filled with 40 mbar H_2 gas, as indicated at the bottom (right axis) of Fig. 4(b). The change in the light intensity with the cyclic variation of the H_2 gas pressure was monitored using the MOKE apparatus. As Fig. 1(c) shows, when the analyzer angle was set at approximately -1.5° , the light intensity in a vacuum was greater than that in H_2 gas. Therefore, as shown in Fig. 4(b), after exposure to 40 mbar

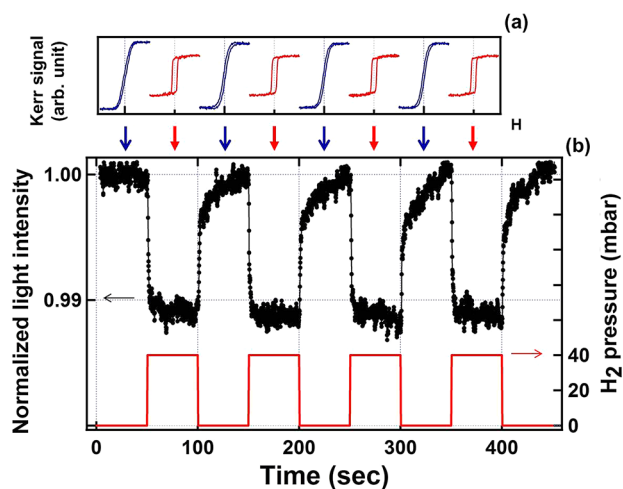


FIG. 4. Reversible variations of the (a) hysteresis loops and (b) light intensity (left axis) for the 14 nm $\text{Co}_{14}\text{Pd}_{86}/\text{Al}_2\text{O}_3(0001)$ alloy film, measured for cyclic exposure to 40 mbar H_2 gas. The maximum switching magnetic field in (a) is ± 500 Oe. The red solid lines (right axis) at the bottom of (b) indicate the H_2 pressure during the measurement.

H₂, the light intensity dropped to a minimum within 3 s. Immediately after pumping out the H₂ gas, the light intensity recovered 60% of the reduction in approximately 2 s, and this was followed by a relatively slow increase with a longer time constant of 20 ± 5 s. The quick response and the delayed part in recovery might be due to the hydrogen desorption from the β -state and α -state, respectively, because of the different bonding strength in β -PdH and α -PdH.³⁰ In Fig. 4(a), MOKE hysteresis loops corresponding to the different H₂ pressures are plotted. The reversibility of the effect of hydrogenation on the magnetic properties can be clearly observed.

In summary, the reversible effect of hydrogenation on magnetism was investigated in Pd-rich alloy film: Co₁₄Pd₈₆/Al₂O₃(0001). The presence of hydrogen atoms in the interstitial sites between Co and Pd atoms mediated the long-range ordered magnetic coupling in the Pd-rich alloy film, which was indicated by a drastic increasing in the squareness of hysteresis loops from approximately 10% to 100% and by a pronounced enhancement of the magnetic coercivity by a factor of nearly 10. In addition, after exposure to 1000 mbar H₂, the saturation Kerr signal was appreciably reduced to nearly 30% of the pristine value in a vacuum, inferring a reduction of the magnetic moment. This study demonstrates the critical manipulation of magnetism of the Co₁₄Pd₈₆ alloy films through the reversible control of the electronic structure; the reversible control was achieved through cyclic exposure to H₂ gas. Similar effects are expected to be observed in various Pd-rich magnetic alloy films and these results will be valuable in future applications of hydrogen sensors and spintronic devices.

This study was financially sponsored by Ministry of Science and Technology, Taiwan under Grant Nos. NSC 102-2112-M-003-003-MY3, NSC 102-2923-M-003-002-MY3, and NSC 102-2112-M-018-006-MY3.

¹D. Sander, W. Pan, S. Ouazi, J. Kirschner, W. Meyer, M. Krause, S. Müller, L. Hammer, and K. Heinz, *Phys. Rev. Lett.* **93**, 247203 (2004).

²B. Busiakiewicz and I. Zasada, *Phys. Rev. B* **78**, 165412 (2008).

³C. C. Kuo, W. C. Lin, S. F. Chuang, and M.-T. Lin, *Surf. Sci.* **576**, 76 (2005).

⁴D. Chiba, M. Sawicki, Y. Nishitani, Y. Nakatani, F. Matsukura, and H. Ohno, *Nature* **455**, 515 (2008).

⁵D. Wang, K.-Y. Lee, S. Luo, and T. B. Flanagan, *J. Alloys Compd.* **252**, 209 (1997).

⁶L. L. Jewell and B. H. Davis, *Appl. Catal., A* **310**, 1–15 (2006).

⁷Z. Zhao, M. A. Carpenter, H. Xia, and D. Welch, *Sens. Actuators, B* **113**, 532–538 (2006).

⁸F. J. Ibanñez and F. P. Zamborini, *J. Am. Chem. Soc.* **130**, 622–633 (2008).

⁹C. S. Chang, M. Kostylev, and E. Ivanov, *Appl. Phys. Lett.* **102**, 142405 (2013).

¹⁰D. Lederman, Y. Wang, E. H. Morales, R. J. Matelon, G. B. Cabrera, U. G. Volkman, and A. L. Cabrera, *Appl. Phys. Lett.* **85**, 615 (2004).

¹¹E. A. Gonzalez, P. V. Jasen, N. J. Castellani, and A. Juan, *J. Phys. Chem. Solids* **65**, 1799–1807 (2004).

¹²S. Akamaru, T. Matsumoto, M. Hara, K. Nishimura, N. Nunomura, and M. Matsuyama, *J. Alloys Compd.* **580**, S102–S104 (2013).

¹³R. Delmelle and J. Proost, *Phys. Chem. Chem. Phys.* **13**, 11412 (2011).

¹⁴W. C. Lin, C. S. Chi, T. Y. Ho, and C. J. Tsai, *Thin Solid Films* **531**, 487–490 (2013).

¹⁵W. C. Lin, C. S. Chi, T. Y. Ho, C. J. Tsai, F. Y. Lo, H. C. Chuang, and M. Y. Chern, *J. Appl. Phys.* **112**, 63914 (2012).

¹⁶W. C. Lin, C. J. Tsai, B. Y. Wang, C. H. Kao, and W. F. Pong, *Appl. Phys. Lett.* **102**, 252404 (2013).

¹⁷K. Munbodh, F. A. Perez, C. Keenan, D. Lederman, M. Zhernenkov, and M. R. Fitzsimmons, *Phys. Rev. B* **83**, 094432 (2011).

¹⁸W. C. Lin, C. J. Tsai, X. M. Liu, and A. O. Adeyeye, *J. Appl. Phys.* **116**, 073904 (2014).

¹⁹A. Remhof and A. Borgschulte, *ChemPhysChem* **9**, 2440–2455 (2008).

²⁰R. Bardhan, L. O. Hedges, C. L. Pint, A. Javey, S. Whitelam, and J. J. Urban, *Nat. Mater.* **12**, 905–912 (2013).

²¹G. K. Pálsson, A. Bliersbach, M. Wolff, A. Zamani, and B. Hjörvarsson, *Nat. Commun.* **3**, 892 (2012).

²²K. Binder and A. P. Young, *Rev. Mod. Phys.* **58**, 801–925 (1986).

²³L. Sandlund, P. Granberg, L. Lundgren, P. Nordblad, P. Svedlindh, J. A. Cowen, and G. G. Kenning, *Phys. Rev. B* **40**, 869 (1989).

²⁴F. Klose, Ch. Rehm, D. Nagengast, H. Maletta, and A. Weidinger, *Phys. Rev. Lett.* **78**, 1150 (1997).

²⁵B. Hjörvarsson, J. A. Dura, P. Isberg, T. Watanabe, T. J. Udovic, G. Andersson, and C. F. Majkrzak, *Phys. Rev. Lett.* **79**, 901–904 (1997).

²⁶Z. Q. Qiu and S. D. Bader, *Rev. Sci. Instrum.* **71**, 1243–1255 (2000).

²⁷P. K. Kulriya, B. R. Mehta, D. K. Avasthi, D. C. Agarwal, P. Thakur, N. B. Brookes, A. K. Chawla, and R. Chandra, *Appl. Phys. Lett.* **96**, 053103 (2010).

²⁸P. K. Kulriya, B. R. Mehta, D. C. Agarwal, P. Kumar, S. M. Shivaprasad, J. C. Pivin, and D. K. Avasthi, *J. Appl. Phys.* **112**, 014318 (2012).

²⁹C. Desplanches, E. Ruiz, A. Rodríguez-Fortea, and S. Alvarez, *J. Am. Chem. Soc.* **124**, 5197–5205 (2002).

³⁰S. Ohno, M. Wilde, and K. Fukutani, *J. Chem. Phys.* **140**, 134705 (2014).